present work demonstrates that borenium salts are obtained from dibutylboron triflate and 9-(((trifluoromethyl)sulfonyl)oxy)-9-borabicyclo[3.3.1]borane and sterically demanding bases such as 2,6-lutidine while pyridine and 2,4-lutidine form only Lewis acid–Lewis base adducts with these diorganylboranes as well as with dibutylboron chloride and 9-chloro-9-borabicyclo[3.3.1]nonane. Therefore, there is competition between adduct and salt formation. In addition, diorganylborenium cations of type R_2BL^+ (L = pyridine, acridine) can be generated from the adducts $R_2BCl{\cdot}L$ by halide abstraction with $AlCl_3$ or $GaCl_3$, but base exchange between the diorganylboron halide adduct and the halide acceptor is a competing reaction.

Acknowledgment. C.K.N. gratefully acknowledges a Humboldt Fellowship. We are also grateful to Fonds der Chemischen Industrie and BASF-Aktiengesellschaft for support of our work and to Deutsche Forschungsgemeinschaft for providing us with the Bruker WP 200 NMR spectrometer. Thanks are due to Dr. H. Prigge, A. Bittner, D. Schlosser, and F. Dirschl for recording many NMR spectra, as well as to K. Schönauer and L. Moser, who provided elemental analysis.

Registry No. **1a**, 96806-75-6; **1b**, 96806-77-8; **2a**, 96806-78-9; **2b**, 96806-79-0; **2c**, 96806-80-3; **2d**, 96806-81-4; **3**, 96806-83-6; **4**, 96807-01-1; **5**, 96807-02-2; **6**, 96807-03-3; **7a**, 96806-84-7; **7b**, 96806-85-8; **7c**, 96806-86-9; **7d**, 22086-36-8; **7e**, 96806-87-0; **7f**, 96806-88-1; **10**, 13059-59-1; **11a**, 96825-32-0; **11b**, 96806-89-2; **11c**, 96806-90-5; **12**, 96806-92-7; **13**, 96806-93-8; **14**, 96806-95-0; 9-BBN-OTF, 62731-43-5; 9-BBN-Cl, 22086-34-6; $GaCl_3$, 13450-90-3; $AlCl_3$, 7446-70-0; dibutylboron triflate, 60669-69-4; 2,6-lutidine, 108-48-5; pyridine, 110-86-1; 2,4-lutidine, 108-47-4; 2,2′-bipyridine, 366-18-7; dibutylboron chloride, 1730-69-4; 9-(((trifluoromethyl)sulfonyl)oxy)-9-borafluorene, 96806-96-1; 9-(((trifluoromethyl)sulfonyl)oxy)-9-borafluorene–pyridine, 96806-97-2; 9-(((trifluoromethyl)sulfonyl)oxy)-9-borafluorene–2,4-lutidine, 96806-98-3; 9-(((trifluoromethyl)sulfonyl)oxy)-9-borafluorene–2,6-lutidine, 96806-99-4; acridine, 260-94-6.

Supplementary Material Available: Tables containing fractional coordinates and isotropic thermal parameters of hydrogen atoms, anisotropic thermal parameters of non-hydrogen atoms, and F_o/F_c values (48 pages). Ordering information is given on any current masthead page.

Contribution from the Department of Chemistry, West Virginia University, Morgantown, West Virginia 26506-6045

Synthesis, Structural Characterization, and Electrochemistry of [1]Metallocenophane Complexes, $[Si(alkyl)_2(C_5H_4)_2]MCl_2$, M = Ti, Zr

CHANDRASEKHAR S. BAJGUR, WAYNE R. TIKKANEN, and JEFFREY L. PETERSEN*

Received November 8, 1984

A series of modified metallocene dichloride compounds, $[SiR_2(C_5H_4)_2]MCl_2$ (M = Ti, R = CH_3; M = Zr, R = CH_3, C_2H_5, n-C_3H_7), have been prepared to evaluate the presence of a dialkylsilyl bridge on their electrochemical behavior. The compounds have been characterized by elemental analysis and ^1H and ^{13}C NMR, and the molecular structures of $[Si(CH_3)_2(C_5H_4)_2]MCl_2$, M = Ti, Zr, have been determined by X-ray diffraction methods. The ^{13}C NMR resonance of the bridgehead carbons is consistently located substantially upfield from the corresponding resonances for the proximal and distal carbons of the rings in these compounds. Cyclic voltammetric measurements have shown that these [1]metallocenophane dichlorides exhibit only one one-electron reversible reduction in THF within a scan range of +1.0 to −3.0 V vs. SCE. Complementary EPR studies were conducted to identify and monitor the stability of the paramagnetic species generated during the electrochemical reduction of $[Si(CH_3)_2(C_5H_4)_2]TiCl_2$ and the sodium naphthalide reduction of $[Si(CH_3)_2(C_5H_4)_2]MCl_2$, M = Ti, Zr. These reduction processes proceed similarly with the formation of only one paramagnetic product, $[Si(CH_3)_2(C_5H_4)_2]MCl_2^-$. The inherent stability observed for these d^1 M(III) monoanions apparently follows directly from the ability of the dimethylsilyl bridge to restrict the mobility of the cyclopentadienyl rings and thereby limit their potential participation in these reduction reactions. The compounds $[Si(CH_3)_2(C_5H_4)_2]MCl_2$, M = Ti, Zr, similarly crystallize in a monoclinic unit cell of $C2/c$ symmetry with the following refined lattice parameters: for M = Ti, a = 13.309 (5) Å, b = 9.871 (2) Å, c = 13.337 (4) Å, β = 132.79 (1)°, V = 1285.8 (7) Å^3, and ρ_{calcd} = 1.576 g/cm^3; for M = Zr, a = 13.391 (3) Å, b = 9.965 (2) Å, c = 10.922 (3) Å, β = 113.37 (2) Å, V = 1337.8 (5) Å^3, and ρ_{calcd} = 1.730 g/cm^3. Full-matrix least-squares refinement (based on F_o^2) converged with respective final discrepancy indices of $R(F_o)$ = 0.024, 0.032 and σ_1 = 1.69, 1.93 for diffractometry data with $F_o^2 > \sigma(F_o^2)$.

Introduction

One of the most widely studied series of electron-deficient, early-transition-metal organometallic compounds is $Cp^*_2MCl_2$, where $Cp^* = C_5H_xMe_{5-x}$, x = 0, 1, 5, and M = Ti, Zr, and its derivatives.[1] The two cyclopentadienyl rings in these compounds and their related derivatives typically display a canted arrangement that forms a protective pocket about the metal center. Under appropriate conditions, various investigators have observed that the Cp^* ligand in these group 4[42] metallocenes can actively participate in many different chemical reactions. These processes include H/D exchange[2] of ring and methyl protons, ring coupling[3] that leads to the formation of a dinuclear fulvalene complex, ring migration[4] with a C_5H_5 unit acting simultaneously as a σ and π donor to two metal centers, and ring detachment[5] that accompanies the formation of a polynuclear metal complex. This widely diverse behavior of the Cp^* ligand, as demonstrated by these aforementioned examples, arises from its inherent ability to venture across the frontier orbital surface of the metal. This premise was demonstrated initially in early-transition-metal chemistry by a classical study performed by Calderon, Cotton, et al.,[6] who ob-

(1) (a) Wailes, P. C.; Coutts, R. S. P.; Weigold, H. "Organometallic Chemistry of Titanium, Zirconium, and Hafnium"; Academic Press: New York, 1974. (b) Bottrill, M.; Gavens, P. D.; Kelland, J. W.; McMeeking, J. "Comprehensive Organometallic Chemistry"; Wilkinson, G., Stone, F. G. A., Abel, E. W., Eds.; Pergamon Press: Oxford, 1982; pp 271–431. (c) Cardin, D. J.; Lappert, M. F.; Raston, C. L.; Riley, P. I. "Comprehensive Organometallic Chemistry"; Wilkinson, G., Stone, F. G. A., Abel, E. W., Eds.; Pergamon Press: Oxford, 1982; pp 549–633.

(2) (a) Bercaw, J. E.; Marvich, R. H.; Bell, L. G.; Brintzinger, H. H. *J. Am. Chem. Soc.* **1972**, *94*, 1219. (b) Bercaw, J. E. *Adv. Chem. Ser.* **1978**, *No. 167*, 136.

(3) (a) Brintzinger, H. H.; Bercaw, J. E. *J. Am. Chem. Soc.* **1970**, *92*, 6182. (b) Davison, A.; Wreford, S. S. *J. Am. Chem. Soc.* **1974**, *96*, 3017. (c) Guggenberger, L. J.; Tebbe, F. N. *J. Am. Chem. Soc.* **1973**, *95*, 7870. (d) Guggenberger, L. J.; Tebbe, F. N. *J. Am. Chem. Soc.* **1976**, *98*, 4137.

(4) (a) Pez, G. P. *J. Am. Chem. Soc.* **1976**, *98*, 8072. (b) Bottomley, F.; Lin, I. J. B.; White, P. S. *J. Am. Chem. Soc.* **1981**, *103*, 703.

(5) Huffman, J. C.; Stone, J. G.; Krussel, W. G.; Caulton, K. G. *J. Am. Chem. Soc.* **1977**, *99*, 5829.

0020-1669/85/1324-2539$01.50/0

served that the two η^5-C_5H_5 rings and the two η^1-C_5H_5 rings of $(\eta^5\text{-}C_5H_5)_2Ti(\eta^1\text{-}C_5H_5)_2$ are fluxional and interchange on the NMR time scale.

A reasonable strategy to reduce the participation of the Cp* ligand in some or all of these side reactions is to link the two rings by an interannular bridge. This stereochemical modification has been employed successfully to alter the reactivity of a number of organometallic compounds. Smith and Brintzinger[7] have reported that titanocene derivatives with an interannular ethylene bridge do not always follow reaction pathways previously observed for the unbridged species, such as the formation of a dinuclear Ti(II) dinitrogen complex, H/D exchange of the ring protons, and the formation of a Ti(III) hydride compound. Marks and co-workers[8] have employed the chelating dicyclopentadienyl ligand $[Si(CH_3)_2(C_5H_4)_2]^{2-}$ to stabilize the $(C_5H_5)_2UCl_2$ configuration with respect to C_5H_5 redistribution. They have further found that the steric congestion introduced by the C_5Me_5 ligand in various bis(pentamethylcyclopentadienyl)thorium compounds can be reduced substantially by a dimethylsilyl bridge.[9] An alternative use of the $[Si(CH_3)_2(C_5H_4)_2]^{2-}$ ligand relates to the synthesis of dinuclear iron complexes, such as $Si(CH_3)_2[(C_5H_4)Fe(CO)_2]_2$, in which the two iron centers are held in close proximity.[10] Subsequent electrochemical studies[10b,c] have shown that the redox behavior of these ring-bridged dimers differs substantially from that of their unbridged analogues.

In view of the demonstrated participation of the Cp* ligand in titanocene and zirconocene chemistry,[11] the use of a chelating bis(cyclopentadienyl) ligand, such as $[Si(CH_3)_2(C_5H_4)_2]^{2-}$, to restrict the mobility of the rings provides an attractive way to minimize other (potentially undesirable) side reactions that lead to ring-coupled or ring-bridged dinuclear products or proceed with the concomitant loss of a Cp* ligand. An additional useful feature of this ligand is that by varying the alkyl substituents on the Si atom one can control the solubility of these modified metallocenes and their derivatives. On the basis of these considerations, an appropriate synthetic scheme for the preparation of $[SiR_2(C_5H_4)_2]MCl_2$, M = Ti, Zr, has been developed. In this paper we wish to report the synthesis and characterization of $[SiR_2(C_5H_4)_2]MCl_2$ (M = Ti, R = CH_3; M = Zr, R = CH_3, C_2H_5, n-C_3H_7). To evaluate the effect of the SiR_2 bridge on the electrochemistry of these [1]metallocenophane dichlorides, cyclic voltammetric measurements have been performed. Complementary EPR studies were undertaken to observe the formation and to evaluate the relative stability of any paramagnetic d^1 M(III) species generated during the electrochemical reduction of $[Si(CH_3)_2(C_5H_4)_2]TiCl_2$ and the sodium naphthalide reduction of $[Si(CH_3)_2(C_5H_4)_2]MCl_2$, M = Ti, Zr. The results from these experiments are contrasted with the corresponding data available for the respective unbridged metallocene dichlorides and clearly demonstrate the ability of the $[SiR_2(C_5H_4)_2]^{2-}$ ligand to stabilize the M(III) oxidation state to further reduction.

Experimental Section

General Procedures. Solvents (reagent grade) were purified and dried by standard methods.[12] The solvents were vacuum distilled into solvent storage flasks containing either $[(\eta^5\text{-}C_5H_5)_2Ti(\mu\text{-}Cl)]_2Zn$[13] (THF, toluene, benzene, DME, pentane) or P_4O_{10} ($CHCl_3$, CH_2Cl_2, CH_3CN) prior to use. The deuterated solvents chloroform-d_1 (Stohler) and benzene-d_6 (Aldrich) were vacuum distilled into appropriate solvent storage containers. Dicyclopentadiene (Eastman, technical grade), dichlorodialkylsilanes, $SiCl_2R_2$ (R = CH_3, C_2H_5, n-C_3H_7) (Petrarch), n-butyllithium and methyllithium (Aldrich), and $TiCl_4$ and $ZrCl_4$ (reaction grade, 99.6%) were used as purchased. Tetra-n-butylammonium hexafluorophosphate (TBAH) was prepared by the metathesis of tetra-n-butylammonium bromide (Alfa) and potassium hexafluorophosphate (Alfa) in ethyl acetate. The compound was recrystallized twice from ethyl acetate and dried in vacuo at 10^{-4} mmHg for 24 h. Reagent grade naphthalene (Eastman) and freshly cut sodium were used to prepare sodium naphthalide.

All manipulations with air- and moisture-sensitive compounds were carried out under a prepurified Ar or N_2 atmosphere in flame-dried glassware on a double-manifold high-vacuum line with use of standard Schlenk techniques or on an all-glass vacuum line fitted with high-vacuum Teflon stopcocks. The handling of solid materials was performed inside a nitrogen-filled inert-atmosphere drybox (Vacuum Atmospheres Co.).

Elemental analyses of $[SiR_2(C_5H_4)_2]MCl_2$ (M = Ti, R = CH_3; M = Zr, R = CH_3, C_2H_5, n-C_3H_7) were performed by Galbraith Laboratories, Inc., Knoxville, TN.

Instrumentation. ^1H and ^{13}C NMR spectra were recorded on a Varian CFT-20 NMR spectrometer operating in the FT mode. Spectra were measured in chloroform-d_1, with the residual ^1H or ^{13}C resonance (δ 7.25[12] and 77.2,[14] respectively, related to Me_4Si) or Me_4Si as the internal standard. Electrochemical measurements were performed with a BAS 100 electrochemical analyzer (Bioanalytical Systems). The cyclic voltammograms were recorded on a DMP-40 series digital plotter (Houston Instruments). EPR spectra were measured with an IBM/Bruker ER 200D EPR spectrometer controlled by an ASPECT computer system. The microwave frequency was monitored with a Hewlett-Packard 5340A frequency counter. The magnetic field of the spectrometer was calibrated by an internal NMR gauss meter (±0.01 G).

Synthesis of $[SiR_2(C_5H_4)_2]MCl_2$ Complexes (M = Ti, R = CH_3; M = Zr, R = CH_3, C_2H_5, n-C_3H_7). The general scheme for the synthesis of these $[SiR_2(C_5H_4)_2]MCl_2$ complexes involves three steps:

$$2NaC_5H_5 + SiR_2Cl_2 \rightarrow SiR_2(C_5H_5)_2 + 2NaCl \quad (1)$$

$$SiR_2(C_5H_5)_2 + 2LiR' \rightarrow Li_2[SiR_2(C_5H_4)_2] + 2R'H \quad (2)$$

$$Li_2[SiR_2(C_5H_4)_2] + MCl_4 \rightarrow [SiR_2(C_5H_4)_2]MCl_2 + 2LiCl \quad (3)$$

R = CH_3, C_2H_5, C_3H_7; R' = CH_3, n-C_4H_9; M = Ti, Zr

This reaction sequence was performed consecutively, and the experimental details are provided below.

a. Preparation of $[Si(CH_3)_2(C_5H_4)_2]TiCl_2$. The procedure employed to prepare $[Si(CH_3)_2(C_5H_4)_2]TiCl_2$ was modified from that described by Kopf.[15] The reaction sequence was performed in a 500-mL three-necked flask fitted with a pressure-equalizing funnel, a nitrogen inlet adapter, and a mechanical stirrer and was initiated by the dropwise addition of 6.4 mL (0.053 mol) of dichlorodimethylsilane into a 150-mL THF solution (−60 °C) containing 9.34 g (0.106 mol) of freshly prepared NaC_5H_5. The reaction mixture was rapidly stirred for 1 h and allowed to warm to room temperature. The reaction flask was then cooled in a n-propyl alcohol/liquid-nitrogen slush bath to −80 °C, and 33.1 mL (0.106 mol) of a 3.2 M solution of n-butyllithium in hexane was added dropwise. The reaction mixture was allowed again to warm to room temperature and stirred for 2 h. Finally, the dilithio salt was added slowly to a second 500-mL three-necked flask containing 10.05 g (0.053 mol) of $TiCl_4$ dispersed in 30 mL of pentane at 0 °C. The reddish brown mixture was stirred at room temperature for several hours, and the solvents were removed. After the residue was washed twice with 20-mL portions of pentane, the pentane-insoluble product was dried and extracted with $CHCl_3$ to give 11.21 g (69.3% yield based on $TiCl_4$) of the product. Large dark red-brown crystals of $[Si(CH_3)_2(C_5H_4)_2]TiCl_2$ were obtained by recrystallization with CH_2Cl_2. Anal. Calcd for $C_{12}H_{14}TiCl_2$ (empirical formula): C, 47.30; H, 4.59. Found: C, 47.19; H, 4.70.

b. Preparation of $[SiR_2(C_5H_4)_2]ZrCl_2$, R = CH_3, C_2H_5, n-C_3H_7. The general synthetic procedure to prepare $[SiR_2(C_5H_4)_2]ZrCl_2$, R = CH_3, C_2H_5, n-C_3H_7, is essentially the same for all three compounds.[16] The

(6) (a) Calderon, J. L.; Cotton, F. A.; Takats, J. *J. Am. Chem. Soc.* **1971**, *93*, 3587. (b) Calderon, J. L.; Cotton, F. A.; DeBoer, B. G.; Takats, J. *J. Am. Chem. Soc.* **1971**, *93*, 3592.
(7) Smith, J. A.; Brintzinger, H. H. *J. Organomet. Chem.* **1981**, *218*, 159.
(8) Secaur, C. A.; Day, V. W.; Ernst, R. D.; Kennelly, W. J.; Marks, T. J. *J. Am. Chem. Soc.* **1976**, *98*, 3713.
(9) Fendrick, C. M.; Mintz, E. A.; Schertz, L. D.; Marks, T. J. *Organometallics* **1984**, *3*, 819.
(10) (a) Weaver, J.; Woodward, P. *J. Chem. Soc., Dalton Trans.* **1973**, 1439. (b) Wegner, P. A.; Uski, V. A.; Kiester, R. P.; Dabestani, S.; Day, V. W. *J. Am. Chem. Soc.* **1977**, *99*, 4846. (c) Wright, M. E.; Mezza, T. M.; Nelson, G. O.; Armstrong, N. R.; Day, V. W.; Thompson, M. R. *Organometallics* **1983**, *2*, 1711. (d) Day, V. W.; Thompson, M. R.; Nelson, G. O.; Wright, M. E. *Organometallics* **1983**, *2*, 494.
(11) Pez, G. P.; Armor, J. N. *Adv. Organomet. Chem.* **1981**, *19*, 1.
(12) Gordon, A. J.; Ford, R. A. "The Chemist's Companion"; Wiley-Interscience: New York, 1972; pp 431–436.
(13) Sekutowski, D. G.; Stucky, G. D. *Inorg. Chem.* **1975**, *14*, 2192.
(14) Levy, G. C.; Lichter, R. L.; Nelson, G. L. "Carbon-13 Nuclear Magnetic Resonance Spectroscopy", 2nd ed.; Wiley-Interscience: New York, 1980; p 30.
(15) (a) Kopf, H.; Kahl, W. *J. Organomet. Chem.* **1974**, *64*, C37. (b) Kopf-Maier, P.; Kahl, W.; Klouras, N.; Hermann, G.; Kopf, H. *Eur. J. Med. Chem.-Chim. Ther.* **1981**, *16*, 275.
(16) An alternative procedure for the preparation of $[Si(CH_3)_2(C_5H_4)_2]ZrCl_2$ has been reported by Yasuda et al.[17]

Table I. Summary of ^1H and $^{13}C\{^1H\}$ NMR Data

compd	^1H NMR		$^{13}C\{^1H\}$ NMR	
	C_5H_4	R	C_5H_4	R
$[Si(CH_3)_2(C_5H_4)_2]TiCl_2$	7.21 (t,[b] 4 H) 5.95 (t, 4 H)	0.75 (s, CH_3, 6 H)	135.51 (4 C_2)[c] 118.78 (4 C_3) 106.78 (2 C_1)	-5.39 (CH_3, 2 C)
$[Si(CH_3)_2(C_5H_4)_2]ZrCl_2$	6.97 (t, 4 H) 5.97 (t, 4 H)	0.75 (s, CH_3, 6 H)	128.60 (4 C_2) 114.29 (4 C_3) 109.17 (2 C_1)	-5.17 (CH_3, 2 C)
$[Si(C_2H_5)_2(C_5H_4)_2]ZrCl_2$	6.96 (t, 4 H) 5.99 (t, 4 H)	1.27 (s,[d] C_2H_5, 10 H)	128.33 (4 C_2) 114.62 (4 C_3) 108.03 (2 C_1)	6.37 (CH_2, 2 C) 1.20 (CH_3, 2 C)
$[Si(C_3H_7)_2(C_5H_4)_2]ZrCl_2$	6.86 (t, 4 H) 5.92 (t, 4 H)	1.05 (m, C_3H_7, 14 H)	128.31 (4 C_2) 114.54 (4 C_3) 108.29 (2 C_1)	18.05 ($SiCH_2$, 2 C) 16.50 (CH_2, 2 C) 12.15 (CH_3, 2 C)

[a] In $CHCl_3$-d_1; chemical shifts (δ) downfield from Me_4Si. [b] $J_{^3H-H}$ = 3 Hz. [c] The numbering system for the C_5H_4 ring is

[d] Apparent singlet.

increased solubility of these [1]zirconocenophane dichlorides that follows as the length of the alkyl chain increases modifies the choice of solvent employed for recrystallization ($[Si(CH_3)_2(C_5H_4)_2]ZrCl_2$, CH_2Cl_2; $[Si(C_2H_5)_2(C_5H_4)_2]ZrCl_2$, benzene; $[Si(n\text{-}C_3H_7)_2(C_5H_4)_2]ZrCl_2$, pentane). If methyllithium rather than *n*-butyllithium is used in these reactions, it should be pointed out that the methyllithium should be free of LiBr. Otherwise, a halogen-exchange reaction leading to the formation of a mixed-halide product, $[SiR_2(C_5H_4)_2]ZrCl(Br)$, will occur.[18] A typical reaction sequence is initiated by adding dropwise 0.050 mol of the appropriate dichlorodialkylsilane to a 150-mL THF solution containing 8.81 g (0.100 mol) of NaC_5H_5 at -60 °C. The reaction mixture was allowed to warm to room temperature and then stirred for an additional 1 h. The contents of the reaction flask were then cooled to ca. -80 °C, and 62.5 mL (0.100 mol) of a 1.6 M solution of *n*-butyllithium in hexane was added slowly over a period of 1 h. After it was stirred for 30 min, the reaction mixture was warmed to room temperature. A 75-mL DME solution containing 11.65 g (0.05 mol) of $ZrCl_4$ was transferred to the addition funnel and then slowly added to the slurry of the dilithio salt, which had been cooled in an ice bath at 0 °C. The pale yellow reaction mixture was stirred overnight and then gently refluxed at 50 °C for 2 h prior to the removal of the solvents. The product residue was washed with small portions of cold pentane and then extracted and recrystallized with the appropriate solvent to give pale yellow or colorless crystals.

$[Si(CH_3)_2(C_5H_4)_2]ZrCl_2$: 8.1 g (46.5% yield based on $ZrCl_4$). Anal. Calcd for $C_{12}H_{14}SiZrCl_2$ (empirical formula): C, 41.36; H, 4.05. Found: C, 41.50; H, 4.15.

$[Si(C_2H_5)_2(C_5H_4)_2]ZrCl_2$: 9.6 g (51.0% yield). Anal. Calcd for $C_{14}H_{18}SiZrCl_2$ (empirical formula): C, 44.66; H, 4.82. Found: C, 44.63; H, 4.93.

$[Si(n\text{-}C_3H_7)_2(C_5H_4)_2]ZrCl_2$: 8.2 g (40.4% yield). Anal. Calcd for $C_{16}H_{22}SiZrCl_2$ (empirical formula): C, 47.38; H, 5.47. Found: C, 47.36; H, 5.76.

NMR Data. The ^1H NMR spectra measured for $[SiR_2(C_5H_4)_2]MCl_2$ (M = Ti, R = CH_3; M = Zr, R = CH_3, C_2H_5, $n\text{-}C_3H_7$) exhibit the characteristic A_2B_2 pattern expected for the cyclopentadienyl ring protons.[19,20] Three carbon resonances are observed for the ring carbons in the corresponding ^{13}C NMR spectra. The upfield location of the bridgehead carbon (C_1) relative to the other ring carbons (C_2, proximal; C_3, distal) has been identified by its relatively low intensity and confirmed by the corresponding NOE gated-decoupled NMR spectra. This arrangement is especially unusual since the corresponding resonance for the bridgehead carbon was observed by Brintzinger and co-workers[20] to be substantially downfield in the methylene-bridged titanium analogues, $[(CH_2)_n(C_5H_4)_2]TiCl_2$, n = 1-3. The remaining ^1H and $^{13}C\{^1H\}$ NMR data and the corresponding assignments for all of the dialkylsilyl-bridged [1]metallocenophane dichlorides that have been prepared are summarized in Table I.

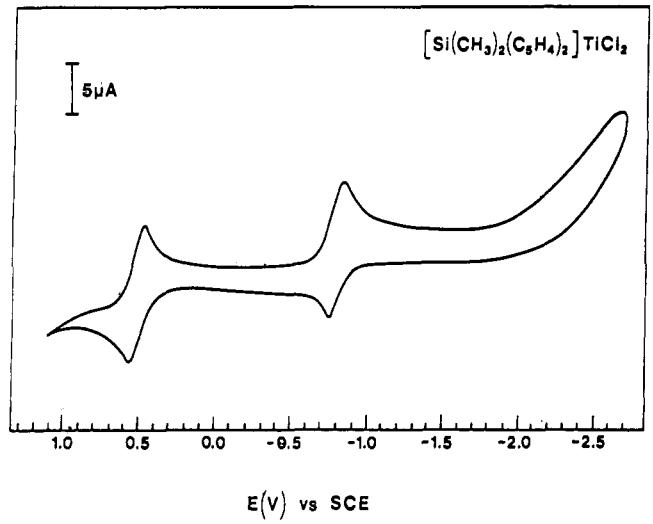

Figure 1. Cyclic voltammogram of $[Si(CH_3)_2(C_5H_4)_2]TiCl_2$ in THF/0.1 M TBAH at a Pt electrode measured with a scan rate of 100 mV/s. The redox wave centered at 0.51 V is due to the ferrocene/ferrocenium couple.

Electrochemical Measurements. Cyclic voltammetric measurements were performed for $[SiR_2(C_5H_4)_2]MCl_2$ (M = Ti, R = CH_3; M = Zr, R = CH_3, C_2H_5, $n\text{-}C_3H_7$) in various solvents including CH_2Cl_2, CH_3CN, and THF. To protect these compounds from exposure to air and moisture, the samples were prepared and the cyclic voltammograms were measured with the electrochemical cell inside a Vacuum Atmospheres drybox. The solution samples were typically 0.1 M TBAH and 1×10^{-3} M in the ring-bridged metallocene dichloride. A single compartment, three-electrode cell was used with a Pt-disk electrode as the working electrode and platinum wires as the auxiliary and reference electrodes. The measured potentials were initially determined relative to that of the internal ferrocenium/ferrocene (1×10^{-3} M) couple and then later corrected to volts vs. SCE for the cyclic voltammograms run in THF. The reduction of ferrocenium to ferrocene is reversible in THF[21] and occurs at E° = 0.51 V vs. SCE under similar conditions.[21b] The scan rates were varied within a range of 20-500 mV/s. The chemical reversibility of an electrochemical process was determined by comparison of the separation between the anodic and cathodic peak potentials to that for internal ferrocene and by the ratio of anodic to cathodic peak currents (i.e. i_a/i_c = 1 for a reversible process).

The cyclic voltammograms obtained for $[SiR_2(C_5H_4)_2]MCl_2$ (M = Ti; R = CH_3; M = Zr, R = CH_3, C_2H_5, $n\text{-}C_3H_7$) indicate that these compounds exhibit only one one-electron reversible reduction in THF. The corresponding cyclic voltammograms for $[Si(CH_3)_2(C_5H_4)_2]TiCl_2$ and $[Si(CH_3)_2(C_5H_4)_2]ZrCl_2$ are depicted in Figures 1 and 2, respectively.

(17) Yasuda, H.; Nagasuna, K.; Akita, M.; Lee, K.; Nakamura, A. *Organometallics* **1984**, *3*, 1470.
(18) (a) Reid, A. F.; Wailes, P. C. *J. Organomet. Chem.* **1964**, *2*, 239. (b) Druce, P. M.; Kingston, B. M.; Lappert, M. F.; Spalding, T. R.; Srivastava, R. C. *J. Chem. Soc. A* **1969**, 2106.
(19) Davis, J. H.; Sun, H.; Redfield, D.; Stucky, G. D. *J. Magn. Reson.* **1980**, *37*, 441.
(20) Smith, J. A.; Seyere, J. V.; Hüttner, G.; Brintzinger, H. H. *J. Organomet. Chem.* **1979**, *173*, 175.
(21) (a) Holloway, J. D. L.; Geiger, W. E., Jr. *J. Am. Chem. Soc.* **1979**, *101*, 2038. (b) Finke, R. G.; Gaughn, G.; Voegeli, R. *J. Organomet. Chem.* **1982**, *229*, 179.

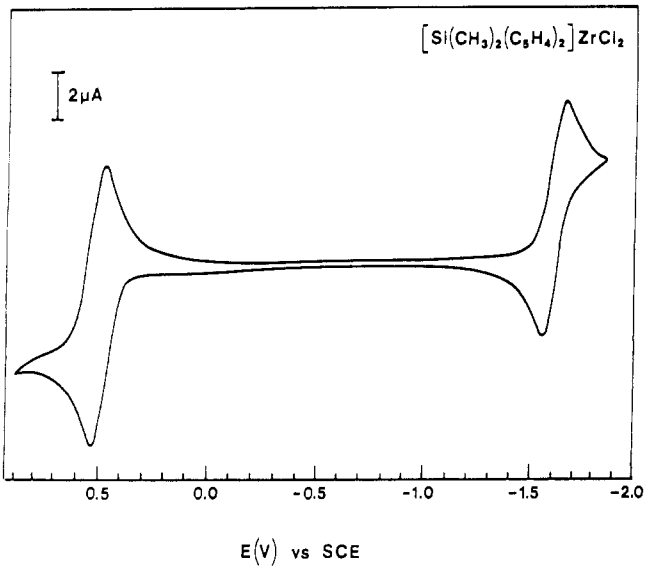

Figure 2. Cyclic voltammogram of $[Si(CH_3)_2(C_5H_4)_2]ZrCl_2$ in THF/0.1 M TBAH at a Pt electrode measured with a scan rate of 100 mV/s. The redox wave centered at 0.51 V is due to the ferrocene/ferrocenium couple.

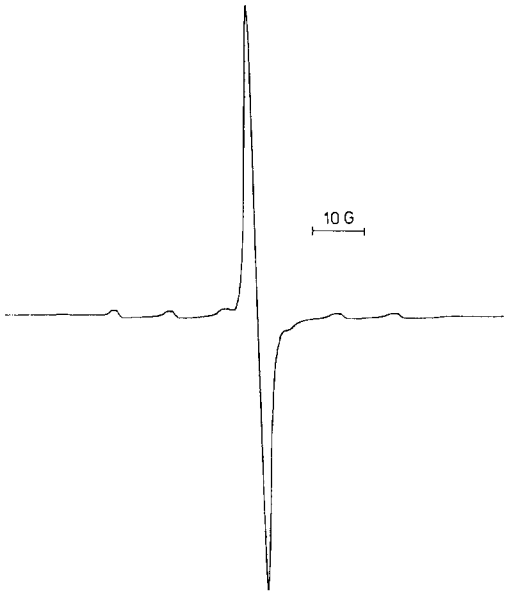

Figure 3. Solution EPR spectrum of in situ electrochemical reduction of $[Si(CH_3)_2(C_5H_4)_2]TiCl_2$ in THF/0.1 M TBAH.

Table II. Reduction Potential Data for $[SiR_2(C_5H_4)_2]MCl_2$, M = Ti, Zr, and Related Complexes

complex	E^0, V vs. SCE	ref
$[Si(CH_3)_2(C_5H_4)_2]TiCl_2$	−0.793[a]	this work
$[Si(CH_3)_2(C_5H_4)_2]ZrCl_2$	−1.600[a]	this work
$[Si(C_2H_5)_2(C_5H_4)_2]ZrCl_2$	−1.602[a]	this work
$[Si(C_3H_7)_2(C_5H_4)_2]ZrCl_2$	−1.603[a]	this work
$(C_5H_5)_2TiCl_2$	−0.800	19b
$(C_5H_5)_2ZrCl_2$	−1.800	19b

[a] Potentials were measured in THF with use of internally referenced Cp_2Fe^+/Cp_2Fe couple, E^0 = 0.51 V vs. SCE, as the internal standard and were calculated from the average of E_{p_c} and E_{p_a}.

An examination of the corresponding cyclic voltammograms of $[Si(C_2H_5)_2(C_5H_4)_2]ZrCl_2$ in CH_3CN and CH_2Cl_2 reveals that the reversibility of this electrochemical process is strongly dependent on the solvent. In this case the reduction is quasi-reversible in CH_3CN and irreversible in CH_2Cl_2. The measured formal potentials, E°, for the $[SiR_2(C_5H_4)_2]MCl_2$ compounds in THF are compared to the corresponding potentials for $(\eta^5\text{-}C_5H_5)_2MCl_2$[21] in Table II.

EPR Measurements. In situ EPR spectra were measured for the paramagnetic species generated during the electrolysis of a THF solution containing 1×10^{-3} M $[Si(CH_3)_2(C_5H_4)_2]TiCl_2$ and 0.1 M TBAH. The solution was placed in a Wilmad flat quartz electrochemical EPR cell equipped with a platinum-gauze working electrode and two platinum wires as auxiliary and reference electrodes. After the cell was properly oriented in the resonance cavity of the EPR spectrometer, a constant potential of ca. −2.0 V vs. SCE was applied and the strength of the EPR signal in Figure 3 increased with time.

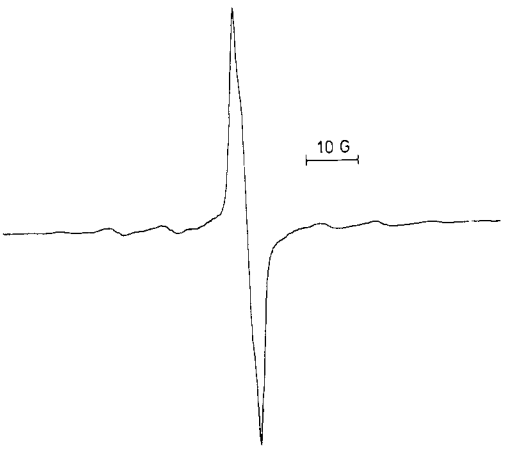

Figure 4. Solution EPR spectrum of sodium naphthalide reduction of $[Si(CH_3)_2(C_5H_4)_2]TiCl_2$ in THF.

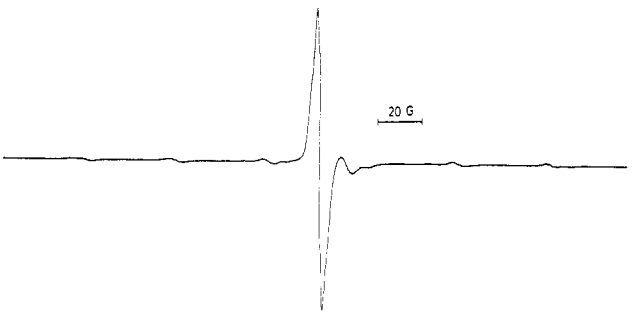

Figure 5. Solution EPR spectrum of sodium naphthalide reduction of $[Si(CH_3)_2(C_5H_4)_2]ZrCl_2$ in THF.

Table III. Summary of Isotropic EPR Parameters

reagent	type of redn	g	A, G
$[Si(CH_3)_2(C_5H_4)_2]TiCl_2$	electrolysis in 0.1 M TBAH/THF	1.9819	$A(^{47}Ti)$ = 12.3
$[Si(CH_3)_2(C_5H_4)_2]TiCl_2$	sodium naphthalide in THF	1.9811	$A(^{47}Ti)$ = 11.3
$[Si(CH_3)_2(C_5H_4)_2]ZrCl_2$	sodium naphthalide in THF	1.9813	$A(^{91}Zr)$ = 42.0

The corresponding chemical reductions of $[Si(CH_3)_2(C_5H_4)_2]MCl_2$, M = Ti, Zr, with sodium naphthalide were similarly monitored by EPR methods. These reactions were performed in a modified quartz EPR tube equipped with a Teflon stopcock and a side-arm reaction bulb. A predetermined amount of sodium naphthalide and a small excess of $[Si(CH_3)_2(C_5H_4)_2]MCl_2$ were placed in the bulb, and several milliliters of THF was vacuum distilled onto the reactants. The reaction mixture was stirred at −20 °C for several minutes, and the solution EPR spectrum was measured to monitor the progress of each reaction.

Since the principal isotopes of Ti and Zr possess a nuclear spin, I, equal to zero, no hyperfine coupling for these nuclei is observed and the solution EPR spectra are each characterized by one predominant line. The small observable distortions superimposed on this line in both Figures 4 and 5 presumably arise from ^1H hyperfine coupling (ca. 0.5 G) of the unpaired electron with the ring protons of the $[Si(CH_3)_2(C_5H_4)_2]^{2-}$ ligand and thereby provide good evidence that the rings remain bound to the metal in these d^1 paramagnetic Ti(III) and Zr(III) species. Additional satellite lines due to the hyperfine coupling of the unpaired electron with either the ^{47}Ti ($I = {}^5/_2$, 7.75%) and ^{49}Ti ($I = {}^7/_2$, 5.51%) nuclei or the ^{91}Zr ($I = {}^5/_2$, 11.23%) nucleus are well resolved in the respective spectra. Since $A(^{47}Ti)$ and $A(^{49}Ti)$ are comparable in magnitude, the intensities of the two outermost hyperfine lines are accordingly weaker than the inner six lines, which contain contributions to their intensity from both of these Ti nuclei. Each metal-based radical in solution was characterized by an isotropic g value, which was calculated from the microwave

Table IV. Data for the X-ray Diffraction Analyses of $[Si(CH_3)_2(C_5H_4)_2]MCl_2$, M = Ti, Zr

	M = Ti	M = Zr
	(A) Crystal Data	
cryst data	monoclinic	monoclinic
space group	$C2/c$ (C_{2h}^6, No. 15)	$C2/c$ (C_{2h}^6, No. 15)
a, Å	13.309 (5)	13.391 (3)
b, Å	9.871 (2)	9.965 (2)
c, Å	13.337 (4)	10.922 (3)
β, deg	132.79 (1)	113.37 (2)
vol, Å^3	1285.8 (7)	1337.8 (5)
mol wt	305.14	348.46
density (calcd)	1.576	1.730
Z, molecules/cell	4	4
μ, cm^{-1}	11.6	12.6
	(B) Data Collection and Analysis Summary	
cryst dimens, mm	0.425 × 0.275 × 0.225	0.325 × 0.138 × 0.200
reflcns sampled	$3 < 2\theta < 50°$ ($\pm hkl$)	$3 < 2\theta < 50°$ ($\pm hkl$)
2θ range for centered reflcns	29.8–35.0	30.5–34.8
scan-width parameters	$A = 1.1$, $B = 0.7$	$A = 1.1$, $B = 0.8$
cryst decay	none	none
total no. of measd reflcns	1202	1249
unique data used ($F_o^2 > \sigma(F_o^2)$)	1106	1136
agreement between equiv data		
R_{av} (F_o)	0.006	0.017
R_{av} (F_o^2)	0.009	0.027
transmission coeff	0.735–0.783	0.790–0.847
P	0.03	0.03
$R(F_o)$	0.024	0.032
$R(F_o^2)$	0.040	0.060
$R_w(F_o^2)$	0.064	0.076
σ_1, error of observn of unit wt	1.69	1.93
no. of variables	103	114
data/parameter ratio	10.7	10.0

frequency and the magnetic field of the central line. The values for the isotropic g values and the metal hyperfine coupling constants are summarized in Table III.

X-ray Structure Analysis of $[Si(CH_3)_2(C_5H_4)_2]MCl_2$, M = Ti, Zr. A crystalline sample of each compound was sealed under an inert atmosphere in a thin-walled capillary tube and transferred to a Picker goniostat that is computer controlled by a Krisel Control diffractometer automation system. Analogous procedures[22] were employed to determine the lattice parameters and to collect the X-ray diffraction data. Duplicate reflections, previously corrected for absorption[23] and Lorentz–polarization effects, were averaged. Specific details regarding the lattice parameters and the data collection procedure are summarized in Table IV.

The initial coordinates for the metal atom in each case were interpreted from the Harker peaks of an unsharpened three-dimensional Patterson map and were used in subsequent Fourier summations to locate the remaining non-hydrogen atoms. In both crystal lattices the metal and silicon atoms lie on a crystallographic twofold rotation axis. Difference Fourier maps calculated with low-angle data ($(\sin\theta)/\lambda < 0.40$ Å^{-1}) were employed to determine reasonable coordinates for the hydrogen atoms. Full-matrix refinement[24-28] (based on F_o^2) with anisotropic temperature factors for the nine non-hydrogen atoms and isotropic temperature factors for the seven hydrogen atoms led to the values for the final discrepancy indices listed in Table IV. A difference electron density map in each case confirmed the completeness of the structural analysis.

Table V. Positional Parameters for $[Si(CH_3)_2(C_5H_4)_2]MCl_2$, M = Ti, Zr[a]

atom	x	y	z
	$[Si(CH_3)_2(C_5H_4)_2]TiCl_2$		
Ti	0.0	0.06929 (4)	1/4
Cl	0.06788 (5)	0.21939 (5)	0.17478 (5)
Si	0.0	−0.27603 (6)	1/4
C1	0.1249 (2)	−0.1416 (2)	0.3715 (2)
C2	0.2038 (2)	−0.0633 (2)	0.3571 (2)
C3	0.2483 (2)	0.0550 (2)	0.4358 (2)
C4	0.1956 (2)	0.0551 (2)	0.4954 (2)
C5	0.1163 (2)	−0.0636 (2)	0.4541 (2)
MeC	0.0612 (3)	−0.3745 (2)	0.1824 (3)
H2	0.226 (3)	−0.086 (3)	0.309 (3)
H3	0.293 (3)	0.130 (3)	0.438 (3)
H4	0.200 (3)	0.118 (3)	0.550 (3)
H5	0.070 (2)	−0.092 (2)	0.479 (2)
MH1	0.040 (5)	−0.461 (4)	0.165 (5)
MH2	0.012 (4)	−0.360 (3)	0.098 (4)
MH3	0.145 (4)	−0.367 (3)	0.229 (3)
	$[Si(CH_3)_2(C_5H_4)_2]ZrCl_2$		
Zr	0	0.17967 (4)	1/4
Cl	0.14945 (7)	0.01931 (9)	0.32688 (10)
Si	0	0.51578 (12)	1/4
C1	0.0035 (3)	0.3871 (3)	0.1276 (3)
C2	0.0959 (3)	0.3117 (3)	0.1383 (4)
C3	0.0614 (4)	0.1965 (4)	0.0579 (4)
C4	−0.0497 (4)	0.1966 (4)	0.0005 (4)
C5	−0.0878 (3)	0.3119 (3)	0.0434 (3)
MeC	0.1266 (4)	0.6140 (5)	0.3147 (5)
H2	0.174 (3)	0.329 (3)	0.192 (4)
H3	0.106 (3)	0.132 (5)	0.053 (4)
H4	−0.091 (4)	0.139 (4)	−0.043 (4)
H5	−0.159 (4)	0.332 (4)	0.015 (5)
MH1	0.112 (8)	0.713 (11)	0.274 (12)
MH2	0.152 (10)	0.647 (14)	0.397 (13)
MH3	0.180 (7)	0.559 (9)	0.315 (10)
MH1′	0.155 (8)	0.643 (12)	0.255 (10)
MH2′	0.117 (11)	0.697 (14)	0.347 (18)
MH3′	0.184 (8)	0.573 (12)	0.401 (11)

[a] The estimated standard deviations in parentheses for this and all subsequent tables refer to the least significant figures.

The positional parameters for all of the atoms from the last least-squares cycle are provided in Table V. Selected interatomic distances and angles and their esd's, which were calculated from the estimated standard errors of the fractional coordinates, are summarized in Table VI. Tables of refined thermal parameters, specific least-squares planes, and the observed and calculated structure factors of $[Si(CH_3)_2(C_5H_4)_2]MCl_2$, M = Ti, Zr, are available as supplementary material.[29]

Discussion of Results

Synthesis of $[SiR_2(C_5H_4)_2]MCl_2$, M = Ti, Zr. The three-step reaction sequence following (1), (2), and (3) provides a convenient method for the preparation of $[SiR_2(C_5H_4)_2]MCl_2$, M = Ti, Zr, in good yield. Although the basic synthetic methodology used to prepare each of these compounds is the same, the choice of solvents employed for extraction and recrystallization purposes varies substantially due to the significantly different solubility properties of these [1]metallocenophane dichlorides. For example,

(22) Jones, S. B.; Petersen, J. L. *Inorg. Chem.* **1981**, *20*, 2889.
(23) The absorption corrections were performed with the use of the general polyhedral shape routine of the program DTALIB. This distance from the crystal center to each face and the corresponding orientation angles (ϕ and χ) required to place each face in diffracting position were provided to define the crystal's shape, size, and orientation with respect to the diffractometer's coordinate system.
(24) The least-square refinement[25] of the X-ray diffraction data was based upon the minimization of $\sum w_i|F_o^2 - S^2F_c^2|$, where w_i is the individual weighting factor and S is the scale factor. The discrepancy indices were calculated from the expressions $R(F_o) = \sum||F_o| - |F_c||/\sum|F_o|$, $R(F_o^2) = \sum|F_o^2 - F_c^2|/\sum F_o^2$, and $R_w(F_o^2) = [\sum w_i|F_o^2 - F_c^2|^2/\sum w_i F_o^4]^{1/2}$. The standard deviation of an observation of unit weight, σ_1, equals $[\sum w_i|F_o^2 - F_c^2|/(n-p)]^{1/2}$, where n is the number of observations and p is the number of parameters varied during the last refinement cycle.
(25) The scattering factors employed in all of the structure factor calculations were those of Cromer and Mann[26] for the non-hydrogen atoms and those of Stewart et al.[27] for the hydrogen atoms with corrections included for anomalous dispersion.[28]
(26) Cromer, D. T.; Mann, J. *Acta Crystallogr., Sect. A: Cryst. Phys., Diffr., Theor. Gen. Crystallogr.* **1968**, *A24*, 231.
(27) Stewart, R. F.; Davidson, E. R.; Simpson, W. T. *J. Chem. Phys.* **1965**, *42*, 3175.
(28) Cromer, D. T.; Liberman, D. J. *J. Chem. Phys.* **1970**, *53*, 1891.
(29) The computer programs that were used for the X-ray diffraction data analysis are described in: Petersen, J. L. *J. Organomet. Chem.* **1979**, *155*, 179.

Table VI. Interatomic Distances (Å) and Bond Angles (deg) for Non-Hydrogen Atoms of $[Si(CH_3)_2(C_5H_4)_2]MCl_2$, M = Ti, Zr[a]

A. Interatomic Distances

	M = Ti	M = Zr
M–Cl	2.356 (1)	2.435 (1)
M–C1	2.379 (2)	2.472 (3)
M–C2	2.366 (2)	2.473 (5)
M–C3	2.436 (2)	2.545 (5)
M–C4	2.432 (2)	2.542 (4)
M–C5	2.356 (2)	2.471 (3)
M–Cp(c)[b]	2.075 (5)	2.197 (6)
Si–MeC	1.849 (4)	1.839 (5)
Si–C1	1.868 (2)	1.866 (4)
C1–C2	1.418 (4)	1.413 (6)
C2–C3	1.404 (3)	1.407 (5)
C3–C4	1.372 (5)	1.367 (7)
C4–C5	1.414 (3)	1.410 (6)
C5–C1	1.410 (4)	1.418 (5)

B. Bond Angles

	M = Ti	M = Zr
Cl–M–Cl*	95.75 (4)	97.98 (4)
Cp(c)–Zr–Cp(c)*	128.7 (1)	125.4 (3)
C1–Si–C1*	89.5 (1)	93.2 (2)
MeC–Si–MeC*	116.6 (2)	115.7 (3)
C1–Si–MeC	111.7 (1)	111.8 (2)
Si–C1–C2	125.0 (2)	125.2 (2)
Si–C1–C5	124.7 (2)	124.6 (3)
C5–C1–C2	105.6 (2)	105.9 (3)
C1–C2–C3	109.0 (3)	108.8 (3)
C2–C3–C4	108.2 (2)	108.3 (4)
C3–C4–C5	108.3 (2)	108.7 (3)
C4–C5–C1	108.8 (3)	108.2 (4)

[a] The esd's given in parentheses for the interatomic separations and bond angles were calculated from the standard errors in the fractional coordinates of the corresponding atomic positions. [b] Cp(c) denotes the ring centroid, and the asterisk (*) denotes the symmetry-related atom.

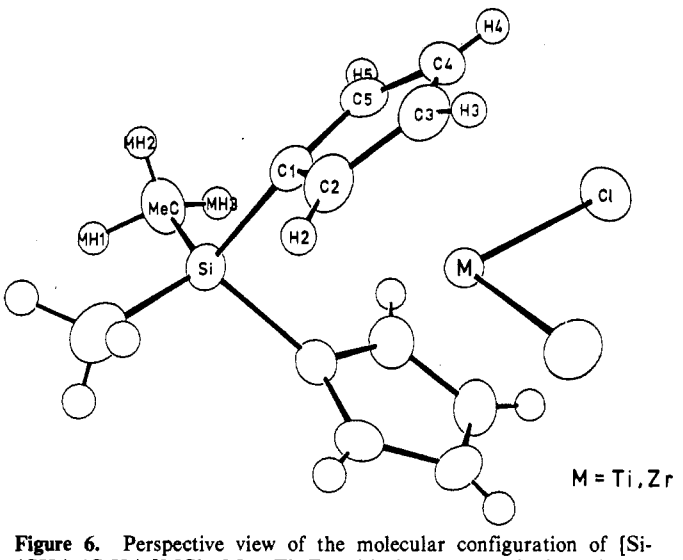

Figure 6. Perspective view of the molecular configuration of $[Si(CH_3)_2(C_5H_4)_2]MCl_2$, M = Ti, Zr, with the atom-numbering scheme. The thermal ellipsoids are scaled to enclose 50% probability.

whereas the dimethylsilyl-bridged derivative of $[SiR_2(C_5H_4)_2]ZrCl_2$ is sparingly soluble in polar solvents such as $CHCl_3$, the ethyl- and *n*-propyl-substituted analogues are reasonably soluble in benzene and pentane, respectively. This observed variation in solubility clearly supports our original contention that it should be possible to alter the solubility of these compounds by varying the alkyl substituents on the Si.

Description of the Molecular Structures for $[Si(CH_3)_2(C_5H_4)_2]MCl_2$, M = Ti, Zr. The molecular structures of $[Si(CH_3)_2(C_5H_4)_2]TiCl_2$ and $[Si(CH_3)_2(C_5H_4)_2]ZrCl_2$ have been determined by X-ray diffraction methods. A perspective view of their molecular structure is provided in Figure 6 with the appropriate atom-labeling scheme. Although their crystal lattices are not isomorphous, the observed structure in each case is constrained by the presence of a crystallographic twofold rotation axis, which bisects the Cl–M–Cl′ bond angle and passes through the metal and Si atoms.

Table VII. Available Structural Data for Metallocene and [1]Metallocenophane Dichlorides of Group 4 Metals

ref	compd	θ, deg[a]	M–Cl, Å	ϕ, deg[b]
28	$(C_5H_4CH_3)_2TiCl_2$	53.3	2.361 (2)	130.2
18	$[CH_2(C_5H_4)_2]TiCl_2$	63, 68	2.34 (1) av	121, 122
18	$[C_2H_4(C_5H_4)_2]TiCl_2$	53	2.350 (1)	128.2
30	$[C_3H_6(C_5H_4)_2]TiCl_2$	46.4		133
this work	$[Si(CH_3)_2(C_5H_4)_2]TiCl_2$	51.2	2.356 (1)	128.7 (1)
29	$(C_5H_4CH_3)_2ZrCl_2$	54.2	2.443 (1), 2.442 (1)	128.9 (2)
31	$[C_3H_6(C_5H_4)_2]ZrCl_2$	50.2	2.431 (2), 2.450 (1)	129
this work	$[Si(CH_3)_2(C_5H_4)_2]ZrCl_2$	56.8	2.435 (1)	125.4 (3)
32	$[C_3H_6(C_5H_4)_2]HfCl_2$	49.4	2.417 (3), 2.429 (2)	129.5

[a] θ is defined as the dihedral angle between the planes of the cyclopentadienyl rings. [b] ϕ is the ring centroid–M–ring centroid angle.

The molecular parameters about the central metal atom are comparable to those reported for $(\eta^5\text{-}C_5H_4CH_3)_2MCl_2$ (M = Ti,[30] Zr[31]) and other group 4 [1]metallocenophane dichlorides (Table VII).[20,32-34] These systems are characterized by a pseudotetrahedral ligand arrangement about the metal. The principal modification that arises when the cyclopentadienyl rings are linked together by either a methylene or dimethylsilyl bridge is an alteration in the degree of canting of the rings. On the basis of their structural studies of $[(CH_2)_n(C_5H_4)_2]TiCl_2$ (*n* = 1–3), Brintzinger and co-workers[20] found that as the length of the methylene chain increases, the rings become more parallel (i.e., less canted). This trend is reflected by the parallel decrease and increase in the angles θ and ϕ, respectively. By comparison with these methylene-bridged titanocene dichlorides, it is apparent that the dimethylsilyl bridge in $[Si(CH_3)_2(C_5H_4)_2]TiCl_2$ produces essentially the same degree of ring canting as that observed for its ethylene-bridged analogue, $[C_2H_4(C_5H_4)_2]TiCl_2$. It is also worthy to note that the canting associated with $[Si(CH_3)_2(C_5H_4)_2]MCl_2$, M = Ti, Zr, is comparable to that of the corresponding nonbridged $(\eta^5\text{-}C_5H_4CH_3)_2MCl_2$ compounds, M = Ti, Zr.

An examination of the structural parameters associated with the cyclopentadienyl rings indicates that the dimethylsilyl bridge has introduced several distinct structural alterations. First of all, the average C3–C4 bond distance of 1.37 Å is consistently shorter by ca. 0.04 Å than the remaining C–C bonds within the rings. The greater double-bond character of this bond suggests that the ring carbon atoms do not interact with the metal in a true η^5 fashion. This remark is further supported by the nonplanarity of the rings and by the substantially longer M–C distances for C3 and C4. In $[Si(CH_3)_2(C_5H_4)_2]TiCl_2$ these two atoms are displaced 0.08 Å above the plane passing through C1, C2, and C5 and away from the metal, whereas in $[Si(CH_3)_2(C_5H_4)_2]ZrCl_2$ they are displaced by 0.06 Å in the same direction. Collectively, these three structural modifications indicate that the interaction of the $[Si(CH_3)_2(C_5H_4)_2]^{2-}$ ligand with the metal in these compounds contains a small but noticeable π-bonding contribution from a η^3-allyl η^2-olefin resonance structure.

Comments Regarding Carbon-13 Chemical Shift of the Bridgehead Carbon. An unusual spectral feature associated with these dialkyl-bridged compounds is the relative position of the ^{13}C NMR resonance for the bridgehead carbon atoms (C_1) of the

(30) Petersen, J. L.; Dahl, L. F. *J. Am. Chem. Soc.* **1975**, *97*, 6422.
(31) Petersen, J. L.; Egan, J. W., Jr. *Inorg. Chem.* **1983**, *22*, 3571.
(32) Epstein, E. F.; Bernal, I. *Inorg. Chim. Acta* **1973**, *7*, 211 and references cited therein.
(33) Saldarriaga-Molina, C. H.; Clearfield, A.; Bernal, I. *J. Organomet. Chem.* **1974**, *80*, 79.
(34) Saldarriaga-Molina, C. H.; Clearfield, A.; Bernal, I. *Inorg. Chem.* **1974**, *13*, 2880 and references cited therein.

cyclopentadienyl rings. From the available data provided by Brintzinger and co-workers[20] for the methylene-bridged titanium compounds $[(CH_2)_n(C_5H_4)_2]TiCl_2$, n = 1–3, this resonance for the dialkylsilyl-bridged analogue is expected to appear similarly downfield rather than substantially upfield from the resonances for the proximal and distal carbons of the rings. For example, in the case of $[Si(CH_3)_2(C_5H_4)_2]TiCl_2$ the proximal and distal carbons resonate at δ 135.51 and 118.78, respectively, and are comparably located for $[(CH_2)(C_5H_4)_2]TiCl_2$ at δ 131.3 and 112.8, respectively. In contrast, the bridgehead carbons for $[Si(CH_3)_2(C_5H_4)_2]TiCl_2$ resonate at δ 106.78, which is ca. 40 ppm farther upfield than its corresponding value of δ 145.4 in $[(CH_2)(C_5H_4)_2]TiCl_2$. Since structural studies of these two compounds indicate that the chelating dicyclopentadienyl ligand is disposed about the titanium with the bridging atom similarly displaced by 0.4–0.6 Å out of the plane of the cyclopentadienyl rings, one is led to conclude that the orbital hybridization associated with the σ-bonding framework about the bridgehead carbon is comparable in these systems. This remark suggests that the explanation of this large upfield shift probably depends on various factors which mainly influence the π-electron density distribution within the rings.

A considerable amount of ^{13}C NMR data has been accumulated for monosubstituted ferrocenes by Nesmeyanov and co-workers[35] and for alkyl- and silyl-substituted metallocene dichlorides, $(\eta^5\text{-}C_5H_4R)_2MCl_2$, M = Ti, Zr, Hf, by Lappert and co-workers[36] to investigate the influence of substituent effects on the ^{13}C resonance of the junction carbon of the ring. Their data similarly show that electron-donating substituents such as alkyl and trimethylsilyl reduce the π-electron density at the junction carbon via an internal polarization mechanism and thereby shift its resonance downfield relative to the parent metallocene. For example, the corresponding ^{13}C chemical shifts for the junction carbons of $(\eta^5\text{-}C_5H_4CH_3)_2ZrCl_2$ and $(\eta^5\text{-}C_5H_4SiMe_3)_2ZrCl_2$ are δ 130.1 and 126.4, respectively, and are significantly downfield from the single ^{13}C resonance for $(\eta^5\text{-}C_5H_5)_2ZrCl_2$ at δ 115.7. The replacement of the methyl substituents by trimethylsilyl groups produces a relatively small upfield shift for the junction carbon resonance. An extrapolation of this trend to the corresponding ring-bridged compounds, however, is complicated by the fact that the relative positions of the junction carbons in $(\eta^5\text{-}C_5H_4R)_2MCl_2$ (M = Ti, Zr; R = Me, $SiMe_3$) and the bridgehead carbons in $[Z(C_5H_4)_2]MCl_2$ (Z = CH_2, $SiMe_2$) are quite different. Structural studies of $(\eta^5\text{-}C_5H_4CH_3)_2MCl_2$, M = Ti, Zr[30,31] indicate that the methyl substituents generally reside above and below the MCl_2 moiety in order to minimize their steric interactions. This arrangement places the junction carbons directly above or below the metal atom. Since the cyclopentadienyl rings freely rotate in solution, the measured chemical shift for the junction carbons represents an average of the contributions due to orientation effects. On the other hand, the bridging linkage in $[Z(C_5H_4)_2]MCl_2$ mandates a substantially different orientation for the bridgehead carbons. In this case, their positions are fixed and located away from the MCl_2 portion of the molecule. Consequently, the magnetic anisotropy of the chemical shift tensor of the bridgehead carbons is based on a substantially different spatial arrangement and is expected to be quite sensitive to the electronic effects and stereochemical constraints introduced by the bridging group. This sensitivity is reflected by the unusually large upfield shift for the bridgehead carbon that occurs upon replacement of the CH_2 bridge by the dialkylsilyl bridge in these compounds.

The enhanced shielding of the bridgehead carbon that accompanies this alteration of the bridging group apparently reflects an accumulation of π-electron density at this position. Although the precise mechanism by which this occurs is not entirely clear, it does suggest that the $SiMe_2$ bridge is behaving (at least spectroscopically) as an electron-withdrawing group. It this remark is correct, then these dialkylsilyl-bridged compounds should be easier to reduce than their parent metallocenes. To provide an operational test, complementary electrochemical measurements have been performed.

Electrochemical Studies of $[SiR_2(C_5H_4)_2]MCl_2$, M = Ti, Zr. The cyclic voltammograms measured for all of the $[SiR_2(C_5H_4)_2]MCl_2$, M = Ti, Zr, complexes similarly exhibit only one reversible redox wave in THF at a Pt electrode. The ratios of their peak currents are essentially 1:1 and independent of the scan rate over the range 20–500 mV/s. The peak potential separations of ca. 90–95 mV are comparable to that of the ferrocenium/ferrocene couple and thereby are consistent with a one-electron-transfer process. Multiple scans produce traces that are coincident and provide no indication of sample decomposition or the occurrence of side reactions. Scans run up to a negative potential limit of ca. −3.0 V vs. SCE in THF show no evidence of any other electrochemical process. The corresponding cyclic voltammograms measured in CH_3CN are similar to those observed in THF, except that chemically reversible behavior is observed only at fast scans of greater than 200 mV/s. In contrast, the cyclic voltammograms in CH_2Cl_2 show solely irreversible behavior under both slow- and fast-scanning conditions.

For these ring-bridged compounds the primary electron-transfer process that is consistent with this electrochemical data is shown in reaction 4. The reduction potentials for this reaction (Table

$$[SiR_2(C_5H_4)_2]MCl_2 \underset{-e^-}{\overset{+e^-}{\rightleftharpoons}} [SiR_2(C_5H_4)_2]MCl_2^- \quad (4)$$

II) indicate that the Zr compounds are substantially more difficult to reduce than $[Si(CH_3)_2(C_5H_4)_2]TiCl_2$. This result is not surprising, however, since the metal-based LUMO of the corresponding $(\eta^5\text{-}C_5H_5)_2ZrCl_2$ is higher in energy by several kilocalories per mole relative to that in $(\eta^5\text{-}C_5H_5)_2TiCl_2$.[36] The fact that the reduction potentials for the three $[SiR_2(C_5H_4)_2]ZrCl_2$ compounds are nearly identical indicates the alkyl substituents on the dialkylsilyl bridge have no significant influence on this electron-transfer process.

The presence of the chelating $[SiR_2(C_5H_4)_2]^{2-}$ ligand introduces several significant changes with regard to the reduction behavior of the corresponding unbridged metallocene dichloride. These differences become readily apparent upon comparison of the respective cyclic voltammograms for $(\eta^5\text{-}C_5H_5)_2TiCl_2$[37] and $[Si(CH_3)_2(C_5H_4)_2]TiCl_2$, which were measured under similar conditions in THF. Whereas several reduction waves are observed for $(\eta^5\text{-}C_5H_5)_2TiCl_2$, only one reversible reduction is observed within the same potential range for $[Si(CH_3)_2(C_5H_4)_2]TiCl_2$. The fact that no additional features are observed at more negative potentials for the latter clearly suggests that bridging the cyclopentadienyl rings strongly inhibits further reduction of the Ti(III) species. The origin of this stabilization presumably lies in the ability of the $[SiR_2(C_5H_4)_2]^{2-}$ ligand to restrict the mobility of the cyclopentadienyl rings.

The multiple reduction waves observed in the cyclic voltammogram of $(\eta^5\text{-}C_5H_5)_2TiCl_2$ clearly indicate that other reduced species are electrochemically accessible. This observation is consistent with the available structural and spectroscopic data for various titanocene species produced by the chemical reduction of $(\eta^5\text{-}C_5H_5)_2TiCl_2$. Brintzinger and Bercaw[3] observed that the reaction of $(\eta^5\text{-}C_5H_5)_2TiCl_2$ with Na, Na/Hg, or sodium naphthalide proceeds with the formation of dimeric metal hydride, $(\mu\text{-}\eta^5\text{:}\eta^5\text{-}C_{10}H_8)(\mu\text{-}H)_2(\eta^5\text{-}C_5H_5)_2Ti_2$, in which the two cyclopentadienyl rinns have coupled to form this dinuclear fulvalene complex. Pez[4] has repeated this reduction reaction with potassium naphthalide and reported the isolation of a tetrahydrofuran adduct, $(\eta^5\text{-}C_5H_5)_2Ti(\eta^1\text{:}\eta^5\text{-}C_5H_4)Ti(\eta^5\text{-}C_5H_5)(C_4H_8O)$, in which one cyclopentadienyl ring interacts simultaneously with both titaniums as a η^1 σ donor and a η^5 π donor. The formation of these two unusual titanocene compounds relies on the inherent mobility of the cyclopentadienyl ring(s) to provide reaction pathways that

(35) Nesmeyanov, A. N.; Petrovskii, P. V.; Federov, L. A.; Robas, V. I.; Fedin, E. I. *J. Struct. Chem. (Engl. Transl.)* **1973**, *14*, 42.
(36) Lappert, M. F.; Pickett, C. J.; Riley, P. I.; Yarrow, P. I. W. *J. Chem. Soc., Dalton Trans.* **1981**, 805.
(37) El Murr, N.; Chaloyard, A.; Tiroulet, J. *J. Chem. Soc., Chem. Commun.* **1980**, 446.

reduce the coordinative unsaturation that develops at each low-valent titanium center as these reductions proceed with the loss of the Cl^- ligands.

A rather surprising feature associated with the electrochemical data for these $[SiR_2(C_5H_4)_2]MCl_2$, M = Ti, Zr, compounds is that the dialkylsilyl bridge produces a significantly greater effect on the reduction potentials for the zirconium compounds. The reduction potential measured for $[Si(CH_3)_2(C_5H_4)_2]TiCl_2$ is only a few millivolts more positive than that for the first reduction step of $(\eta^5\text{-}C_5H_5)_2TiCl_2$. In contrast, all of the $[SiR_2(C_5H_4)_2]ZrCl_2$ compounds reduce at potentials that are ca. 200 mV more positive than that of $(\eta^5\text{-}C_5H_5)_2ZrCl_2$. The observed decreases in the magnitude of these reduction potentials are consistent with the suggestion (based on the corresponding ^{13}C NMR data) that the dimethylsilyl bridge acts as a net withdrawing group. As a result the $[SiR_2(C_5H_4)_2]MCl_2$ compounds are more easily reduced than their $(\eta^5\text{-}C_5H_5)_2MCl_2$ analogues. However, this does not explain why the reduction potentials of $[SiR_2(C_5H_4)_2]ZrCl_2$ are affected to a significantly greater extent than that for $[Si(CH_3)_2(C_5H_4)_2]TiCl_2$. Presumably, the explanation lies in the larger size of zirconium and the greater radial extension of its valence orbitals to accommodate more easily the addition of an electron within this rigid molecular structure. However, additional electrochemical data on related [1]metallocenophane dichlorides containing different bridging groups will be needed to sort out the relative importance of various electronic and stereochemical factors that influence the reduction potentials of these compounds.

EPR Studies. Parallel EPR experiments were conducted to characterize the paramagnetic species that are produced by either the electrochemical or chemical reduction of $[Si(CH_3)_2(C_5H_4)_2]MCl_2$, M = Ti, Zr. Since the LUMO for these d^0 Ti(IV) and Zr(IV) compounds is a metal-based orbital,[38] a one-electron reduction is expected to proceed (at least initially) with the formation of the corresponding paramagnetic d^1 M(III) monoanions, $[SiR_2(C_5H_4)_2]MCl_2^-$.

In situ electrolysis of $[Si(CH_3)_2(C_5H_4)_2]TiCl_2$ dissolved in a THF solution containing 0.1 M TBAH as the supporting electrolyte proceeds with the generation of only one paramagnetic species. Its EPR spectrum (Figure 3) is characterized by a strong, single resonance at 1.9819 and contains an appropriate number of weaker satellites due to $^{47,49}Ti$ hyperfine coupling of 12.3 G. The fact that its isotropic g value is less than the free-electron value of 2.0023 reflects the spin–orbit coupling contribution that accompanies the placement of the unpaired electron into an orbital of primarily metal character. The magnitudes of the isotropic g and $A(^{47}Ti)$ parameters are comparable to those reported for $(\eta^5\text{-}C_5H_5)_2TiCl_2^-$, which has been generated by electrolysis (g = 1.9789, $A(^{47}Ti)$ = 13.1 G)[37,39] and by γ irradiation (g = 1.9800, $A(^{47}Ti)$ = 13.5 G)[40] of $(\eta^5\text{-}C_5H_5)_2TiCl_2$.

Comparable EPR measurements were carried out to monitor the formation and stability of any paramagnetic species generated during the chemical reduction of $[Si(CH_3)_2(C_5H_4)_2]MCl_2$, M = Ti, Zr, with sodium naphthalide in THF. Both reactions similarly proceed with the formation of one paramagnetic product that is reasonably stable in THF. For $[Si(CH_3)_2(C_5H_4)_2]TiCl_2$, the EPR spectrum (Figure 4) is nearly identical with that obtained for the corresponding species produced upon electrolysis of $[Si(CH_3)_2(C_5H_4)_2]TiCl_2$. The isotropic magnetic parameters for the former of g = 1.9811 and $A(^{47}Ti)$ = 11.3 G are comparable to those of the latter. Since the observed differences in their magnitudes are most likely attributable to ion-pairing effects arising from the widely different concentrations of the countercation in solution, one can conclude that these paramagnetic Ti(III) species are both probably $[Si(CH_3)_2(C_5H_4)_2]TiCl_2^-$. Similarly for $[Si(CH_3)_2(C_5H_4)_2]ZrCl_2^-$, a single resonance at g = 1.9813 is observed with six additional satellites due to ^{91}Zr hyperfine coupling of 42.0 G. The observation of a strong, stable EPR signal for this Zr(III) species is especially notable since efforts to identify any paramagnetic Zr(III) intermediates generated during the electrochemical[39] or chemical reduction[41] of $(\eta^5\text{-}C_5H_5)_2ZrCl_2$ have been unsuccessful until recently.[43]

Concluding Remarks. Collectively, the results of these cyclic voltammetry and EPR studies of $[SiR_2(C_5H_4)_2]MCl_2$, M = Ti, Zr, have shown that the corresponding d^1 M(III) monoanions are accessible. The inherent stability observed for these paramagnetic species follows directly from the ability of the dialkylsilyl bridge to minimize the mobility of the cyclopentadienyl rings and thereby *maintain* their original canted arrangement and the spatial orientation of the LUMO in which the electron is placed during the reduction process. This structural constraint significantly alters the redox behavior of these modified metallocene dichlorides, as evidenced by the observation of only one reversible electrochemical process. The further appearance of only one paramagnetic species upon the chemical or electrochemical reduction of $[Si(CH_3)_2(C_5H_4)_2]MCl_2$, M = Ti, Zr, strongly supports further efforts to develop appropriate synthetic methods leading to the isolation and complete characterization of stable salts of $[Si(CH_3)_2(C_5H_4)_2]MCl_2^-$. The availability of these paramagnetic Ti(III) and Zr(III) anions should provide suitable starting materials to investigate systematically the influence of the unpaired electron on the reactivity of these and related paramagnetic M(III) derivatives.

Acknowledgment. We thank the National Science Foundation (Grant No. ISP-8011453) and Research Corp. for financial support of this research. Computer time for the analysis of the X-ray diffraction data was provided by the West Virginia Network for Educational Telecomputing. The authors further express their appreciation to Professor Eric A. Mintz for his helpful suggestions regarding the synthesis of the $[SiR_2(C_5H_4)_2]MCl_2$ compounds, to Professor Ronald B. Smart for the use of a BAS 100 electrochemical analyzer, and to Professor William E. Geiger, Jr., for his comments regarding the electrochemical analysis.

Registry No. $[Si(CH_3)_2(C_5H_4)_2]TiCl_2$, 51869-68-2; $[Si(CH_3)_2(C_5H_4)_2]ZrCl_2$, 86050-32-0; $[Si(C_2H_5)_2(C_5H_4)_2]ZrCl_2$, 96688-72-1; $[Si(n\text{-}C_3H_7)_2(C_5H_4)_2]ZrCl_2$, 96666-17-0; $Na[Si(CH_3)_2(C_5H_4)_2]TiCl_2$, 96666-18-1; $Na[Si(CH_3)_2(C_5H_4)_2]ZrCl_2$, 96666-19-2; $[Si(CH_3)_2(C_5H_4)_2]ZrCl(Br)$, 96666-20-5; $[Si(C_2H_5)_2(C_5H_4)_2]ZrCl(Br)$, 96666-21-6; $[Si(n\text{-}C_3H_9)_2(C_5H_4)_2]ZrCl(Br)$, 96666-22-7; $TiCl_4$, 7550-45-0; $ZrCl_4$, 10026-11-6; NaC_5H_5, 4984-82-1; dichlorodimethylsilane, 75-78-5; dichlorodiethylsilane, 1719-53-5; dichlorodipropylsilane, 2295-24-1.

Supplementary Material Available: Tables of refined thermal parameters, hydrogen bond distances, least-squares planes, and observed and calculated structure factors for $[Si(CH_3)_2(C_5H_4)_2]MCl_2$, M = Ti, Zr, and cyclic voltammograms for $[SiR_2(C_5H_4)_2]ZrCl_2$, R = C_2H_5, $n\text{-}C_3H_7$ (17 pages). Ordering information is given on any current masthead page.

(38) (a) Lauher, J. W.; Hoffmann, R. *J. Am. Chem. Soc.* **1976**, *98*, 1729. (b) Petersen, J. L.; Lichtenberger, D. L.; Fenske, R.; Dahl, L. F. *J. Am. Chem. Soc.* **1975**, *97*, 6433.
(39) Dessy, R. E.; King, R. B.; Waldrop, M. *J. Am. Chem. Soc.* **1966**, *88*, 5112.
(40) Symons, M. C. R.; Mishra, S. P. *J. Chem. Soc., Dalton Trans.* **1981**, 2258.
(41) Bajgur, C. S.; Petersen, J. L., unpublished results.
(42) In this paper the periodic group notation is in accord with recent actions by IUPAC and ACS nomenclature committees. A and B notation is eliminated because of wide confusion. Groups IA and IIA become groups 1 and 2. The d-transition elements comprise groups 3 through 12, and the p-block elements comprise groups 13 through 18. (Note that the former Roman number designation is preserved in the last digit of the new numbering: e.g., III → 3 and 13.)
(43) Electrochemical studies by Samuel et al.[44] have led to the characterization of the Zr(III) species produced during the electrochemical reduction of $(\eta^5\text{-}C_5H_5)_2ZrL_2$ (L = Cl, Br, CH_3) in THF.
(44) Samuel, E.; Guery, D.; Vedel, J.; Basile, F. *Organometallics* **1985**, *4*, 1073.